Utilization of TanDEM-X data to identify the potential trigger of the 2018's Sunda Strait Tsunami in Indonesia

W. Tampubolon
UNIBW, Institute of Applied Computer Science
Werner-Heisenberg-Weg 39,
85577, Neubiberg, Munich
winhard.tampubolon@unibw.de

W. Reinhardt
UNIBW, Institute of Applied Computer Science
Werner-Heisenberg-Weg 39,
85577, Neubiberg, Munich
wolfgang.reinhardt@unibw.de

Abstract

The Sunda Strait tsunami swept the coastal area of Java Island in the night of December 22, 2018 local time. The responsible institution i.e. Meteorology and Climatology Agency of Indonesia (BMKG) delivered no immediate tsunami early warning at that time. Therefore people around the west coastal area of Java Island including the touristic area of Tanjung Lesung, Ujung Kulon could not prepare themselves to escape from the tsunami waves reported as 3-4 meter high on the ground.

It is still debatable about what is the exact cause of 2018's Sunda Strait tsunami? The major opinion focused on the increasing eruption activity of Anak Krakatau (Child of Krakatoa). Volcanic mudflow material avalanche was suspected as the primary cause to trigger the high sea wave strengthened by the tidal and seasonal wind condition at that time.

In terms of disaster preparedness and emergency response, Radar Interferometry Techniques can play an important role by generating a Digital Elevation Model (DEM) as an input to Decision Support Systems (DSS). In addition, the techniques of differential Interferometric Synthetic Aperture Radar (D-INSAR/D-IFSAR) can provide the earth surface deformation from time series Radar Datasets.

In this paper, we demonstrate the combination between Time Series DEM Analysis and Ground Displacement detection to demonstrate how the potential trigger of the Sunda Strait Tsunami could be detected. We use the German TanDEM-X Coregistered Singlelook Slant-range Complex (CoSSC) in order to generate DEMs in a high resolution format comparable to the large scale topographical mapping specification in Indonesia. The TanDEM-X data acquisition is based on the bi-static IFSAR approach (DLR, 2012). The basic principle is performing a simultaneous measurement of the same scene and identical doppler spectrum by using 2 sensors, thereby avoiding temporal decorrelation. Subsequently, we also apply the differential IFSAR techniques in order to detect the ground deformation.

Keywords: disaster preparedness, IFSAR, rapid mapping, DEM from TanDEM-X data, Copernicus, DEM from Sentinel 1A

1. Introduction

The occurrences of disasters all over the world has increased the awareness of worldwide institutions to collect and use geospatial information in order to strengthen the capabilities to cope with disaster and to minimize human casualties. Especially in emergency situations up to date geo-information has to be provided timely, with high reliability and without bureaucracy obstacles.

1.1 Ina Tsunami Early Warning System

The Indonesian Tsunami Early Warning System (InaTEWS) is the operation system handed over by the former cooperation initiated after the 2004 Indian Ocean tsunami in a so called German Indonesian Tsunami Early Warning System (GITEWS). Basically it consists of land and sea monitoring components as depicted in Figure 1. The land monitoring part is equipped by mainly Global Positioning System (GPS)/Global Navigation Satellite System (GNSS) and broadband seismometer units while the sea monitoring part is equipped by buoy, tide gauge and ocean bottom units. As the corresponding legislation Act Nr.31/2009 stated that Meteorology and Climatology Agency of Indonesia (BMKG) is responsible to deliver the tsunami early warning, InaTEWS is well maintained essentially by BMKG.

Figure 1: InaTEWS components

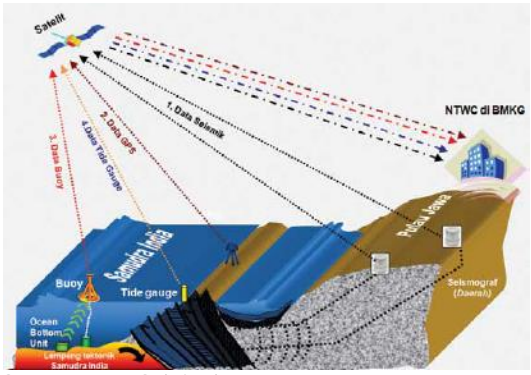

Source: BMKG (2012)

Normally, a tsunami is triggered by the seabed movement following the earthquakes beforehand. Therefore the primary input to be encountered in the InaTEWS is the earthquake detected by the broadband Seismometer units. Even though not detected by BMKG, German's GEOFON Program published an earthquake occurrence just around 1 hour before the tsunami hit the coastal area (Figure 2). The epicentre of this earthquake was located in the Krakatau Island only 4 km from the erupted volcano with the magnitude of 5.1 (Mw).

The Sunda Strait tsunami occurred at around approximately 21 o'clock in the night of December 22, 2018 local time swept west coastal area of Java Island as well as southern coastal area of Sumatra Island. The Indonesian Disaster Management Agency (BNPB) reported 437 casualties, 14,059 injured, 33,721 fled not including the material loss resulted. At that time, there was no tsunami early warning given, only some warning about high tides a day before in the context of sea navigation.

1.2 Background and Objectives

In disaster and emergency situations, geospatial data play an important role to be used within Decision Support Systems (DSS). One fundamental component of the geospatial datasets is the Digital Elevation Model (DEM), which is mandatory in order to enable Geographical Information System (GIS) analysis within quite a number of societal challenges such as demographic changes, marine research and natural hazards. The increasing exploitation of marine resources develops many new coastal settlement areas with a great danger of natural hazard potential at the same time.

Especially within Earthquake / Tsunami events it is a challenge to derive an up to date and not too costly terrain representation through DEMs. Satellite-based radar data are very well suited to fulfill such needs. A wide coverage and flexible data acquisition modes make radar satellite-based data very interesting also for DEM generation especially for large monitoring areas. The main reason for this is the weather independence and high orbit altitudes which can avoid local restrictions and limitations.

We are motivated to identify the potential trigger of the aforementioned disaster by utilizing the radar interferometry techniques (see chapter 2 for details). Hence, our objective is to confirm the contribution of the underwater avalanche to the Sunda Strait tsunami. We use TanDEM-X data to generate a DEM data for the time before the disaster and Sentinel 1A data for the time after the disaster (no TanDEM-X data available for this point in time). Further we estimate the volume through the ground deformation detected (see below).

Figure 2: Earthquake occurrence prior to the Sunda Strait Tsunami

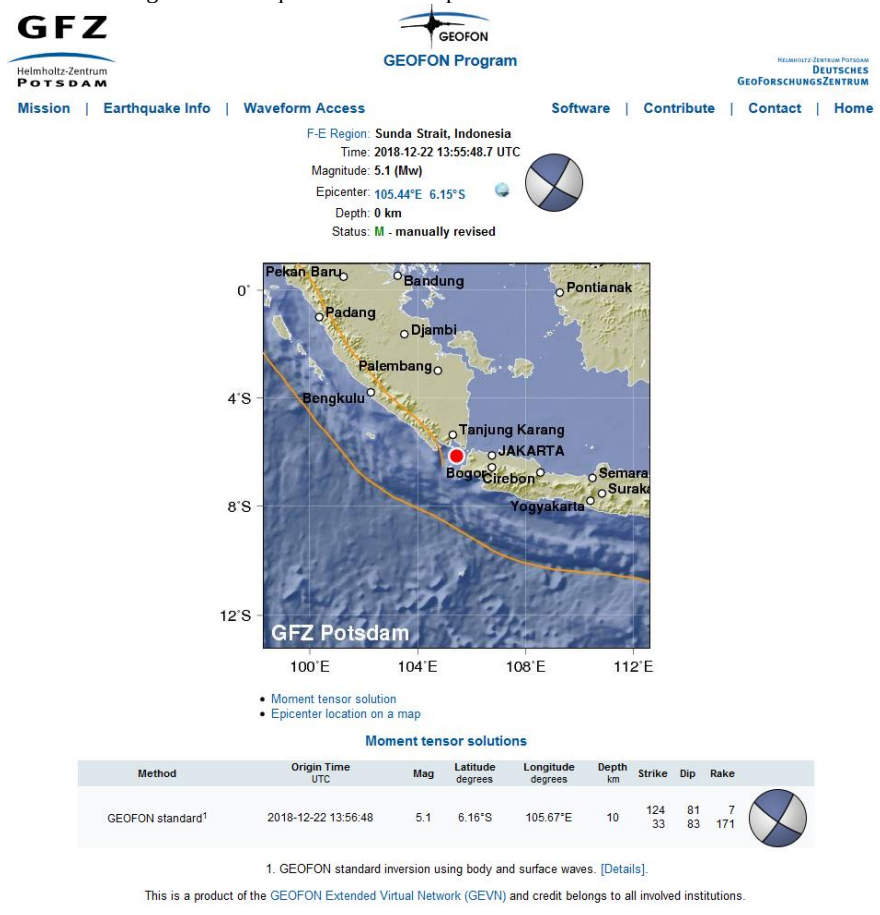

Source: GEOFON Program, GFZ Potsdam-Germany.

In addition, we assume that the underwater landslides resulted from the eruption of Anak Krakatau have a direct contribution to the tsunami wave on the coastal area of Java and Sumatra. By performing some GIS Analysis such as Map Overlay and Volume Calculation, we compare the volume of underwater avalanche from Anak Krakatau with the volume of the inundation area on the coast. From a technical point of view there is another goal of this paper, namely to present a workflow for deriving a DEM from TanDEM-X Radar Interferometric data.

2. TanDEM-X Mission

The TanDEM-X Mission will hopefully provide a global uniform DEM in a resolution of 10-12 m in similar way as the SRTM global DEM in 2001, but with better height accuracy. For our Area of Interest (AOI), TanDEM-X products i.e. Coregistered Singlelook Slant-range Complex (CoSSC) data have been used as a raw dataset to perform the DEM generation as well as the earth surface deformation detection using the interferometric approach (DLR, 2012).

Figure 2: Area of Interest

Source: Bing Imagery, Geospatial Reference System of Indonesia (SRGI), GEOFON Program

To get the CoSSC data, there is a TanDEM-X Data Access Service available only for scientific purposes with a limited Area of interest (AOI). For the AOI as depicted in Figure 2, there are only 2 datasets available as included in Table 1. Unfortunately, the more recent data set is not available.

Table 1: TanDEM-X CoSSC Data (*Height of Ambiguity).

Scenes	HOA* / Baseline (m)	Looking Direction	Acquisition Date
S01	77.185 / 100.514	Descending	21-01-2016
S02	93.483 / 83.207	Descending	14-10-2015

In order to comply with the High Resolution Terrain Information (HRTI) Level 3 standard of National Geospatial-Intelligence Agency (NGA), the height ambiguity must be in the order less than 40 m (Krieger, 2005). In most cases, it is difficult to fulfil this requirement without further improvement as it will be discussed in 2.1.

2.1 DEM Generation

In this section, the workflow of the IFSAR DEM generation for TanDEM-X CoSSC data is briefly described as depicted in Figure 3. Part 1 focuses on the phase unwrapping step as it iteratively improves the results by the output from Part 2 i.e. adjusted baseline value. Part 2 has the objective to convert the unwrapped phase into elevation/height as the final output to construct the DEM.

For the processing of the Radar interferometry data, we use the open source Sentinel Application Platform (SNAP) which is the next generation of the Next ESA SAR Toolbox (NEST) focusing on radar interferometry and polarimetry (Veci, 2016). SNAP desktop is already designed to deal with the TanDEM-X CoSSC (TDM). The steps for the IFSAR DEM generation using SNAP desktop are the following:

1. Interferogram formation of the CoSSC data (TDM format)
   This step provides an interferogram from the pair wise bi-static data acquisition. In order to get only the topographical phase, the flat earth phase must be subtracted.
2. Goldstein filtering
   The objective of the Goldstein filtering is to reduce the number of inaccurate fringes from the interferogram.
3. Multilooking
   The interferogram multilooking step is necessary to increase the positional accuracy of the intensity and wrapped phase by increasing the number of looking views of the CoSSC data. Normally, 2-5 looking views are the optimal solution to produce effective ground range pixels.
4. Export to SNAPHU (Statistical-Cost Network-Flow Algorithm for Phase Unwrapping)
   Currently, the complicated phase unwrapping built-in step is still not provided by the SNAP desktop. Nevertheless, SNAP has an export functionality to hand over the task to the SNAPHU platform.
5. Phase Unwrapping in SNAPHU
   Phase unwrapping using SNAPHU consumes a lot of Random Access Memory (RAM) during processing. Therefore as a rule of thumb, it is necessary to subset the

whole area into a size of less than 20 Megabyte of Wrapped Phase Interferogram.

6. Unwrapped Phase to Elevation
   The Elevation (height) calculation in SNAP is mainly based on a DEM reference e.g. SRTM 1 Arc Second as an existing topographic phase reference. Hence, the absolute phase offset is determined by the DEM reference accuracy.
7. Geocoding
   The geocoding in SNAP considers the terrain correction as well as the input of Ground Control Points (GCPs) if available. However, only planimetric (X,Y) information from the GCPs can be taken into account in the geocoding step.

The previous baseline phase offset estimation result using phase offset functions (POF) from (Mura, 2012) indicates a vertical accuracy in the level of sub meter (2.768 m) by using OrbiSAR X-Band data. This result motivates us to improve the vertical accuracy in TanDEM-X data by taking into account GCP/DEM Reference data in the subsequent linear phase offset estimation using SNAP desktop. For the accuracy assessment, we measure the RMSE of each generated point other than the reference area with the best available DEM (FGDC, 1997).

Figure 3: DEM Generation Workflow

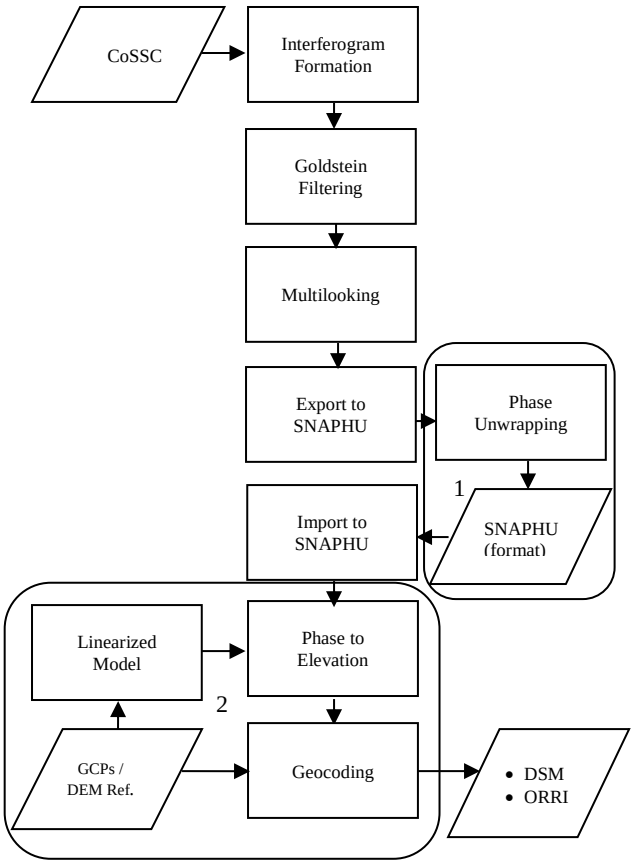

2.2 Differential Interferometric SAR

Differential IFSAR can be applied by using time series radar data to detect earth surface deformation especially in the situation where accurate DEM reference and/or GCP are not available.

$$\Phi = \Phi_{flat} + \Phi_{height} + \Phi_{differential} \quad (1)$$

From equation (1), the differential phase component can be subtracted from unwrapped phase ($\boldsymbol{\Phi}$) if the flat earth phase and height phase are known (Richards, 2007). Afterwards the deformation (d) in meter from multi temporal datasets can be calculated using equation (2), where $\boldsymbol{\lambda}$ = wavelength in m (X Band).

.

$$d = \frac{\lambda \Phi_{differential}}{4\pi} \quad (2)$$

3. Discussion of the approach

Our approach employs time series radar data in order to determine the preliminary analysis of recent Sunda Strait tsunami by performing GIS analysis on TanDEM-X data using toolboxes in ArcGIS desktop.

Under International Charter on Space and Major Disaster, the available space-based data shall be collaboratively distributed by the participating agencies on a voluntary basis after the activation charter on December, 23rd, 2018 in conjunction with the occurrence of Sunda Strait tsunami. This activation made available some post-disaster maps as well as the vector data immediately after Sunda Strait tsunami. In this short paper, some of these GIS vector data are used to support GIS analysis in section 3.1.

3.1 DEM Analysis

As explained in 2.1, the unwrapped Phase to Elevation step needs either GCPs or a DEM reference in order to determine the absolute phase offset by using a linear model adjustment. Therefore we had to extent the model, to introduce three important parameters perpendicular baseline, height reference and phase offset. This extension was already published in an ISPRS Archives publication in 2018 (Tampubolon, 2018).

Currently, only one Geodetic Control Point is available at Anak Krakatau Volcano as depicted in Figure 2 i.e. KTAU. Since it is difficult to conduct the GCP measurements or produce high resolution DEM especially around this active volcano, the alternative strategy in the Unwrapped Phase to Elevation step must be defined. In addition, the phase discontinuities which decrease the height accuracy have to be considered. These phase discontinuities occur due to the sea (waterbody) area.

Basically, as also depicted in Figure 2, there are 3 islands detected surrounding the active volcano i.e. Sertung (West), Krakatau Kecil (East), Krakatau (South). Assuming there is no significant land change in Sertung Island, we use this area as a reference area for the unwrapped Phase to Elevation step. However, as we see in Figure 4, the effect of phase

discontinuities make other islands, including Anak Krakatau, floating away after the height calculation.

To correct this problem, the preliminary condition about the zero height coastlines is added to the processing scheme.

Figure 4: Effect of phase discontinuities (upper part : not corrected, lower part : corrected)

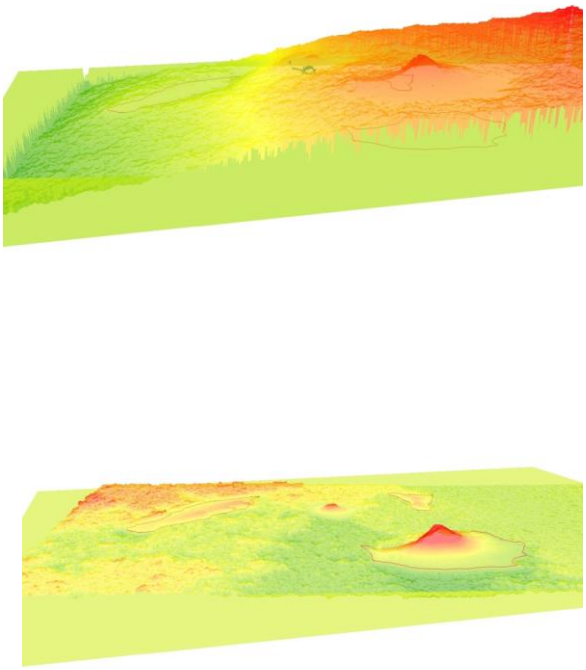

Since our model is linear as formed in (Tampubolon, 2018), the height reference can be shifted from one to another area once the relative heights are fixed.

To estimate the change in volume of the Anak Krakatau volcano we generated DEMs for the time before and after the disaster using the sources given in Table 2 and calculated the volume using the Polygon Volume tool in ArcGIS. The results show a growth in volume between 1999/2000 and 2016 because of continuous minor volcano activities and a clear loss in volume of more than 100 Mio m^3 between 2016 and 2019 (after the tsunami) as also seen in Figure 5.

Table 2: Volume calculation of Anak Krakatau

DEM	Area (Ha)	Volume (m^3)	Acquisition time
SRTM	270.5	154 118 000	1999-2000
TanDEM-X	305.3	243 528 000	21-01-2016
Sentinel 1A	318.8	116 250 000	24-01-2019 12-01-2019
Sentinel 1A	243.2	115 806 000	05-02-2019 24-01-2019

Vector data from Copernicus EMS Rapid Mapping (Copernicus Emergency Management Service, 2018) indicating situations before and after the disaster clearly show that the Anak Krakatau volcano changed his shape enormously after the eruption of December 2018. Part of the former volcano area now is covered by water (called underwater avalanche in Figure 6). Using this vector data we were also able to calculate the lost volume of the volcano, by using the DEM from 2016. It shows that the volcano lost around 44 Mio m^3 (18%) of the volume (Table 3). This is less than the loss calculated from the DEMs, but probably the volcano lost volume also in other areas.

Figure 5: 3 D Visualization of Anak Krakatau (upper part: TanDEM-X 21-01-2016, middle part: Sentinel 1A 05-02-2019, lower part: UAV Photo)

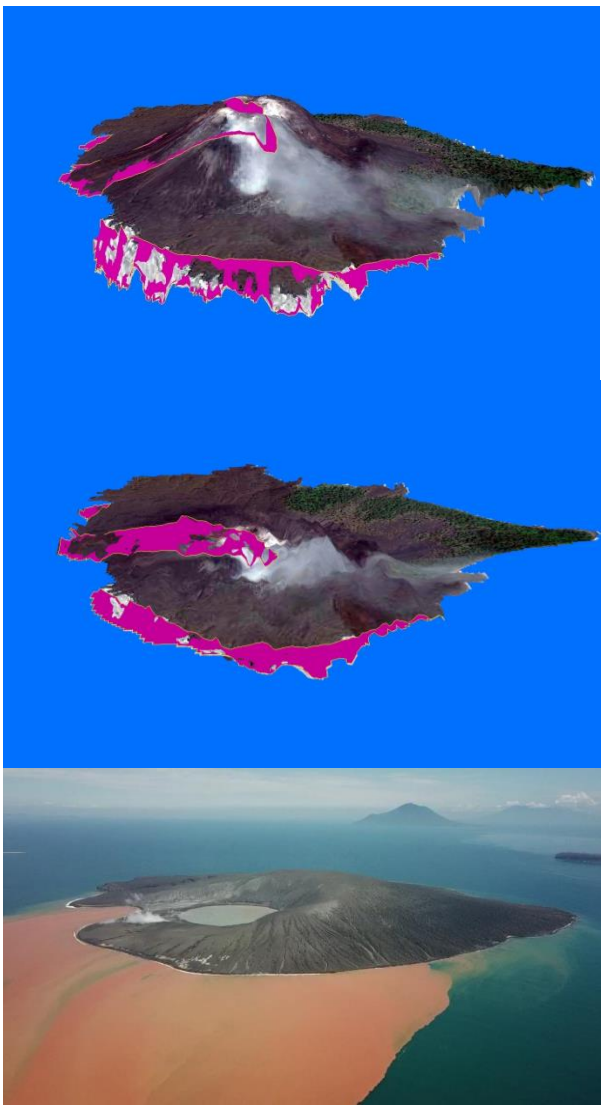

Source: UAV Photo from BNPB

Also from the Copernicus EMS source mentioned above indicating flood trace for the affected area, we have got the coverage of inundation areas after the tsunami. The volume calculation for these inundation areas show a water volume of around 15 Mio m^3 using the SRTM DEM.

Table 3: Volume calculation of lost volcano area

DEM	Area (Ha)	Volume (m^3)	Acquisition time
TanDEM-X	43.39	43 868 000	26-01-2016

By comparing the lost volume of the volcano from Table 3 with the total volume of the inundation areas from Table 4, we are convinced that the inundation was caused by the loss of mass of the Anak Krakatau. The inundation volume is smaller than the volume lost by the volcano, but parts of the water was surely going elsewhere.

Table 4: Volume of inundation area

Area	Area (Ha)	Volume (m^3)
Tanjung Lesung	90.73	3 627 000
Teluk Lada	79.58	2 246 000
Carita Beach	36.13	715 000
Labuhan South	74.49	1 711 000
Labuhan North	42.00	666 000
Taman Agung	60.56	2 122 000
Kalianda	24.42	457 000
Anyer North	37.97	1 118 000
Anyer South	34.08	808 000
Lampung East	10.26	298 000
Lampung West	24.81	736 000
Sumur	33.87	667 000
TOTAL	**548.90**	**15 171 000**

3.2 Ground Displacement Detection

As CoSSC format is a co-registered slave data to the master in a bi-static acquisition mode, the identification of the master dataset is mandatory. The TanDEM-X platform consists of two satellites namely TanDEM-X (TDX) and TerraSAR-X (TSX). For our datasets, we get the information from the included metadata that all the TDX data is a master data set.

By using multi temporal interferometric data processing between 2015 and 2016, the differential phase has been extracted to calculate deformation using equation (2). As shown in Figure 6, the northern and eastern parts of the volcano have more deformation in the range of 20-30 cm (increase). On the other side of the volcano, the deformations were less detected in the range 0-20 cm.

This unequal geodynamic movement of northern and southern parts of Anak Krakatau probably triggered the underwater landslides in the vulnerable area.

Figure 6: Differential IFSAR result based on TanDEM-X

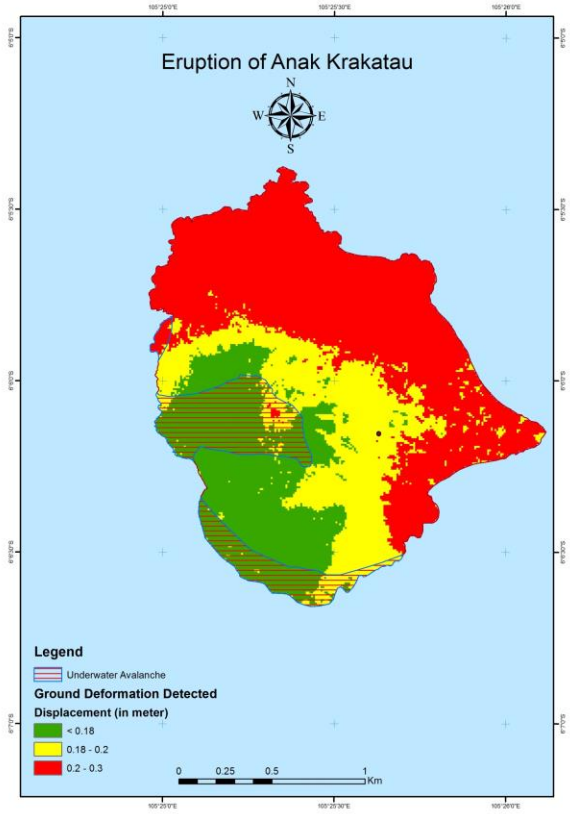

4. Conclusion

We have shown that up-to-date geo data, in this case TanDEM-X data, can play an important role not only in disaster response but also in analysis of causes. Despite neglecting the tidal and current wave factors in our investigations, it is likely that the Sunda Strait tsunami was caused by the eruption activity of Anak Krakatau as depicted in Figure 7 and supported by the results of the investigations in chapter 3.1 and 3.2.

The earthquake occurrence detected by GEOFON was another indication which supports the assumption the tsunami was triggered by the eruption of Anak Krakatau. That means, it is uncertain, but there are clear indicators that the lost masses of the volcano caused the tsunami. Therefore, a bathymetric survey, as already planned in the near future by the responsible institution will probably confirm the underwater terrain changes.

Finally, radar interferometry is a potential technology to be used as a support of the Tsunami Early Warning System (TEWS) not only by DEM Generation but also by differential IFSAR (D-IFSAR) technique. D-IFSAR can be applied especially in the active volcano island in order to monitor the trend of deformation in advance.

Figure 7: Underwater Avalanche Contribution of Anak Krakatau to the Sunda Strait Tsunami

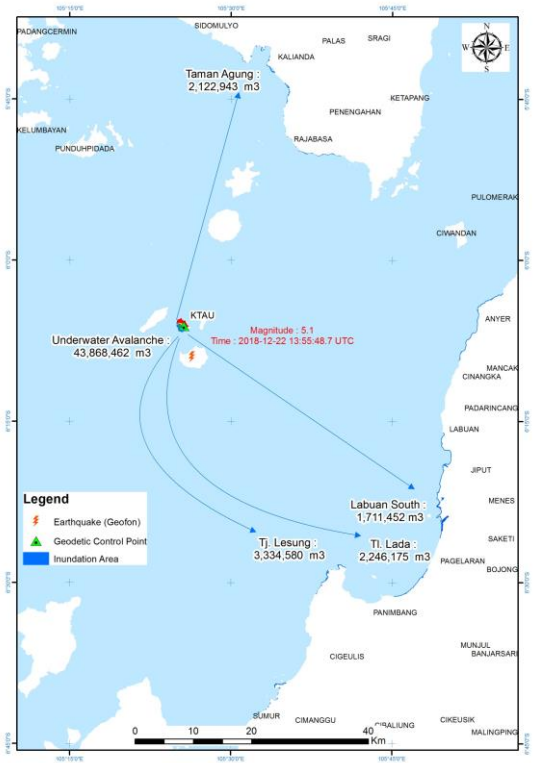

References

BMKG (2012) Guidance Book of Indonesian Tsunami Early Warning System (InaTEWS) Second edition.

Copernicus Emergency Management Service (2018) [EMSR335] Anak Krakatau - INDONESIA: Delineation Map, Monit 01. [Online] Available from: https://emergency.copernicus.eu/mapping/ems-product-component/EMSR335_10ANAKKRAKATAU_01DELINEATION_MONIT01/1 [Accessed 20th February 2019]

DLR (2012) TanDEM-X Payload Ground Segment CoSSC Generation and Interferometric Consideration (version 1.0), Oberpfaffenhofen, Germany, TD-PGS-TN-3129, pp. 20-21.
ESA (2007) InSAR Principle: Guidelines for SAR Interferometry Processing and Interpretation, Noordwijk, The Netherlands, pp. 18-19.

FGDC (1998) Geospatial Positioning Accuracy Standards Part 3: National Standard for Spatial Data Accuracy (version 2.0), Washington, D.C., FGDC-STD-001-1998: Federal Geographic Data Committee, pp.3-4.

Krieger, G., Fiedler, H., Hajnsek, I., Eineder, M., Werner, M., Moreira, A. (2005), TanDEM-X: Mission Concept and Performance Analysis, In: Proceedings of IGARSS 2005. Seoul, Korea.

Mura, J.C., Pinheiro, M., Rosa, R., Moreira, J.R. (2012) A Phase-Offset Estimation Method for InSAR DEM Generation Based on Phase-Offset Functions. In: *Remote Sensing Journal*, ISSN 2072-4292, 745-761.

Veci, L. (2016) Interferometry Tutorial. Array Systems Computing Inc. [Online] Available from https://de.scribd.com/document/353837654/S1TBX-Stripmap-Interferometry-With-Sentinel-1-Tutorial [Accessed 23rd January 2019].

Richards, Mark A. (2007) A Beginner's guide to Interferometric SAR Concepts and Signal Processing. IEEE A&E Systems Magazine Vol.22 No.9.

Tampubolon, W. and Reinhardt, W. (2018) Quality Assessment of an Extended Interferometric Radar Data Processing Approach, In: Int. Arch. Photogramm. Remote Sens. Spatial Inf. Sci., XLII-4, 615-621.